Space Sci Rev (2012) 172:303–314
DOI 10.1007/s11214-011-9749-0

Kinetic Models for Whistler Wave Scattering of Electrons in the Solar Corona and Wind

Christian Vocks

Received: 10 May 2010 / Accepted: 20 January 2011 / Published online: 1 February 2011

Abstract Kinetic models are necessary to describe the physical processes associated with non-Maxwellian velocity distribution functions (VDFs) of electrons or ions in the solar corona and wind. It is shown that pitch-angle scattering of electrons in the solar wind needs to be considered in kinetic solar wind models. Coulomb collisions are not efficient enough to provide this scattering, but resonant interaction with whistler waves is. A solar wind model for undisturbed fast wind is presented, and the influence of scattering on flare electron propagation is investigated. Furthermore, it is found that resonant interaction of electrons with whistler waves is capable of producing suprathermal tails of electron distributions even under quiet conditions without flare activity.

Keywords Solar corona · Solar wind · Kinetic theory · Wave-particle interaction · Electron acceleration · Quasi-linear theory

1 Introduction: Why Kinetic Models?

Fluid descriptions of plasmas are widely used for studies on the origin of the solar wind and the physical processes in the solar corona and interplanetary space. Many models do exist so far, with different degrees of complexity. Examples are two-fluid models, i.e. for protons and electrons, of coronal heating and solar wind acceleration for a given heating function, e.g. Hansteen and Leer (1995), three fluid models adding a heavy ion species, He^{2+} or O^{5+} and heating by Alfvén waves (Ofman 2004), or four-fluid models for both minor ion species and a given turbulence spectrum (Hu et al. 2000). These models describe the solar wind acceleration from the corona up into interplanetary space. The solar wind origin is also investigated by models that focus on the plasma in coronal funnels, e.g. Hackenberg et al. (2000), He et al. (2008).

Describing the plasma or its constituent particle species as a fluid is based on the assumption that the electrons or ions show a collective behavior and thus are effectively coupled.

C. Vocks (✉)
Astrophysikalisches Institut Potsdam, An der Sternwarte 16, 14482 Potsdam, Germany
e-mail: cvocks@aip.de

Their velocity distribution functions (VDFs) are then close to Maxwellian ones, and the whole plasma state is not far away from local thermodynamic equilibrium (LTE). But are these conditions met in the solar corona and wind? As far as Coulomb collisions are concerned, the solar wind is largely collisionless. Only thermal electrons experience some collisions. The solar corona has a higher density, but suprathermal particles are still collisionless. Observations do indeed reveal strong deviations from Maxwellian VDFs. Helios data of solar wind protons (Marsch 2006) show temperature anisotropies and non-Maxwellian VDFs shaped in a way that is in agreement with expectations from resonant interaction with ion cyclotron waves. In the solar corona, strong temperature anisotropies and preferential heating of heavy ions is found (Kohl et al. 1998). Solar wind electron VDFs also show distinct deviations from a Maxwellian, with a thermal core, an isotropic halo of suprathermal electrons, and a magnetic-field aligned beam or "strahl" that is usually directed away from the Sun (Lin 1974; Pilipp et al. 1987).

These non-Maxwellian distributions, their origin and their role in coronal heating and solar wind acceleration are beyond the scope of fluid models. Kinetic models are necessary to describe these processes, like the microphysics of coronal heating and solar wind acceleration. Kinetic models are capable of describing states far away from LTE and provide information on ion and electron VDFs. But a price has to be paid for the kinetic description of the plasma: While fluid models only depend on up to three spatial coordinates, kinetic models also introduce up to three velocity coordinates to describe particle VDFs. This leads to considerably higher computer costs. Furthermore, boundary conditions have to be defined at the bounds of any simulation box, not only in spatial but also in velocity coordinates.

The paper is organized as follows: In the next section, kinetic models for electrons in the solar wind are reviewed and the importance of scattering by resonant interaction with whistler waves is demonstrated. Then, the effect of whistlers on the propagation of flare-generated energetic electrons in interplanetary space is studied. Finally, it is shown that whistler waves can produce suprathermal electrons in a coronal loop even without solar flare activity.

2 Kinetic Models for Electrons in the Solar Wind

Generally, a kinetic model is based on the solution of a Boltzmann-Vlasov equation

$$\frac{\mathrm{d}f}{\mathrm{d}t} = \left(\frac{\partial f}{\partial t}\right)_{\mathrm{diff}} \tag{1}$$

that describes the temporal evolution for the VDF $f(\mathbf{r}, \mathbf{v}, t)$ of one or more particle species. The diffusion term on the right hand side represents e.g. Coulomb collisions or wave-particle interaction. It is 0 for the original Vlasov equation, that describes collisionless particles. The complexity of a kinetic model depends on what physical effects are considered in the term on the right hand side.

2.1 Exospheric Models

The simplest kinetic models are exospheric models (Jockers 1970; Lie-Svendsen et al. 1997) that are based on the assumption that electrons are collisionless above a certain height in the solar atmosphere, called the exobase. Then, solar wind electron VDFs are just described by the Vlasov equation:

$$\frac{\partial f}{\partial t} + (\mathbf{v}\cdot\nabla) f + \left[m_e\gamma\mathbf{g} - e(\mathbf{E} + \mathbf{v}\times\mathbf{B}\right]\cdot\frac{\partial f}{\partial \mathbf{p}} = 0 \tag{2}$$

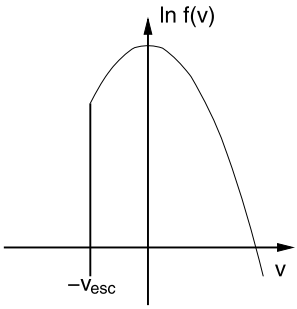

Fig. 1 Sketch of the electron VDF in an exospheric model

g and **E** represent the gravitational and charge separation electric field, respectively, **B** is the background magnetic field, $\gamma = \sqrt{1 + p^2/(m_e c)^2}$ is the Lorentz factor, and m_e is the electron rest mass.

In such a model, suprathermal electrons in the corona exceed the local escape velocity, $v_{\rm esc}$, and thus move into interplanetary space, leading to the formation of a strahl-like structure. However, these electrons escape from the Sun and do not return. So, for negative velocities parallel to the magnetic field $v_\parallel < -v_{\rm esc}$ the VDF becomes $f = 0$ with a sharp cutoff, as illustrated in Fig. 1. The inclusion of Coulomb collisions results in more realistic electron VDFs with a thermal core and an anisotropic halo resembling the strahl (Pierrard et al. 2001), as well as improved solar wind acceleration (Landi and Pantellini 2003). But the steep phase-space gradient at $v_\parallel < -v_{\rm esc}$ remains.

2.2 Suprathermal Tails

Such a gradient is in contrast to observations of an isotropic suprathermal halo (Lin 1974) in the solar wind. The core and halo can be fitted by two Maxwellian VDFs, but even better by a single kappa distribution (Maksimovic et al. 1997)

$$f_\kappa(p) = N_e \frac{\Gamma(\kappa+1)}{\pi^{3/2}(2\kappa-3)^{3/2} p_{th}^3 \Gamma(\kappa-1/2)} \left(1 + \frac{p^2}{(2\kappa-3)\,p_{th}^2}\right)^{-(\kappa+1)} \tag{3}$$

with electron density, N_e, and a "thermal momentum", $p_{th} = \sqrt{m_e k_B T}$. This kappa distribution has power-law suprathermal tails $\propto p^{-2(\kappa+1)}$. The fit can be further improved by a Maxwellian core and a kappa halo (Nieves-Chinchilla and Viñas 2008). Calculating the VDF evolution back to the solar corona shows that a coronal origin of such suprathermal tails is possible (Pierrard et al. 1999).

Such non-Maxwellian coronal electron VDFs have the interesting consequence that nonlocal effects can become important, like velocity filtration (Scudder 1992a, 1992b), and heat fluxes different from the classical Spitzer-Haerm law, even against a temperature gradient (Dorelli and Scudder 2003). Exospheric models with kappa distributions yield more realistic results (Zouganelis et al. 2004) than models based on Maxwellian VDFs, with higher solar wind speeds and electron temperatures. But in these models the problem remains that no electrons with speeds faster than the escape velocity can return to the Sun, so that still $f(v_\parallel < -v_{\rm esc}) \to 0$.

2.3 Electron Scattering in Interplanetary Space

This remains in contrast to observations that indicate not only an anisotropic strahl, but also an isotropic halo. Furthermore, the mirror force in the opening magnetic field structure of

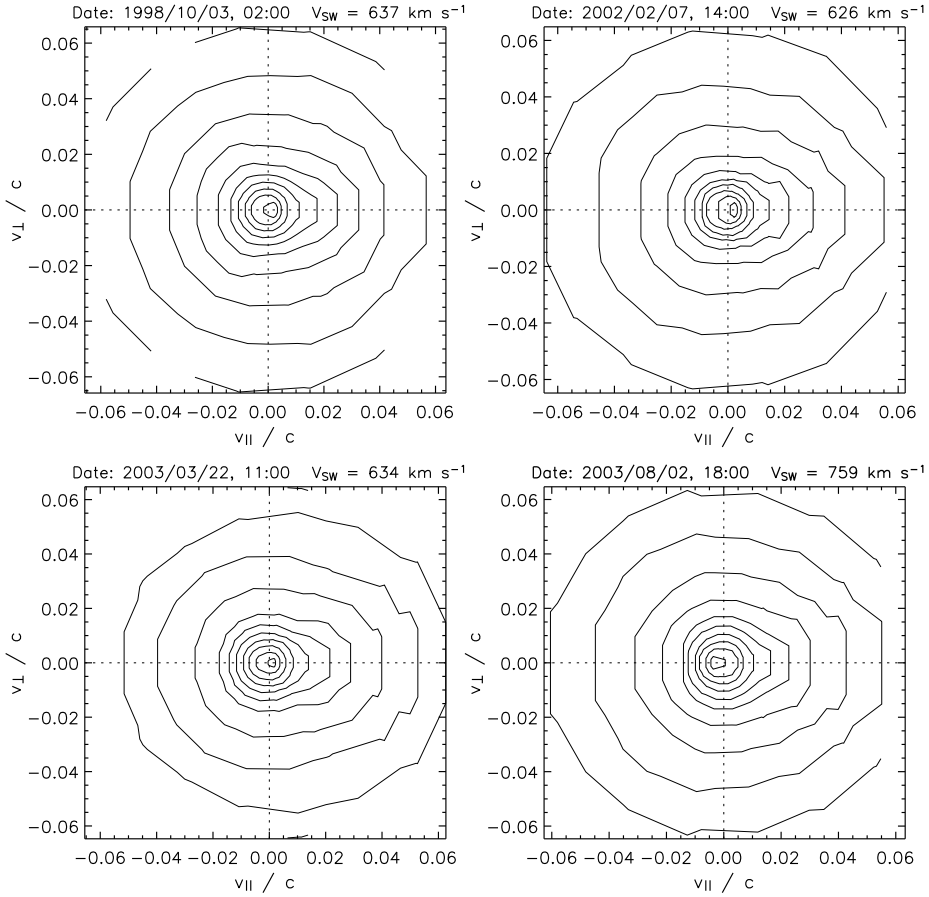

Fig. 2 Solar wind electron VDFs as observed by *WIND* 3DP

the Parker spiral would focus all anti-sunward moving electrons into an extremely narrow beam, which is also not supported by observations of finite strahl widths (Hammond et al. 1996).

Figure 2 shows solar wind electron VDFs as observed by the 3DP instrument onboard the WIND spacecraft (Lin et al. 1995). The core, halo, and strahl populations are clearly visible. For electron energies above 1 keV the distribution becomes isotropic. So some mechanism must exist that scatters electrons back into the anti-solar direction, against the mirror force. Owens et al. (2008) have determined the amount of scattering that is needed from Ulysses observations. Coulomb collisions are too inefficient in interplanetary space, solar wind suprathermal electrons are collision-free.

A promising candidate for this mechanism is electron scattering by electromagnetic waves. Interplanetary space is not a vacuum, but filled with a spectrum of electromagnetic fluctuations (Salem 2000; Mangeney et al. 2001). The cyclotron resonant interaction with whistler waves can be described within the framework of quasilinear theory (Kennel and Engelmann 1966) that, unlike linear theory, describes the long-term evolution of electron VDFs due to wave action but is not fully self-consistent with a prescribed dispersion and being evaluated in the zero wave growth rate limit. The simplifying assumption of wave

propagation parallel to the background magnetic field is made, since otherwise a complicated integral in wave-vector space would result (Marsch and Tu 2001). In the form given by Marsch (1998), the resulting diffusion equation reads in the coordinates momentum, p, and pitch-angle, θ:

$$\left(\frac{\delta f}{\delta t}\right)_{wh.} = \frac{1}{p^2 \sin\theta}\left[\frac{\partial}{\partial p}\left(\alpha_{pp}\frac{\partial f}{\partial p} + \alpha_{p\theta}\frac{\partial f}{\partial \theta}\right) + \frac{\partial}{\partial \theta}\left(\alpha_{\theta p}\frac{\partial f}{\partial p} + \alpha_{\theta\theta}\frac{\partial f}{\partial \theta}\right)\right] \tag{4}$$

with the parameters

$$\begin{aligned} \alpha_{pp} &= \frac{1}{\tau} p^2 \sin^3\theta v_{ph}^2 \\ \alpha_{p\theta} = \alpha_{\theta p} &= \frac{1}{\tau} p \sin^2\theta v_{ph}(v_{ph}\cos\theta - v) \\ \alpha_{\theta\theta} &= \frac{1}{\tau}\sin\theta(v_{ph}\cos\theta - v)^2 \end{aligned} \tag{5}$$

the whistler wave phase speed, v_{ph}, the electron speed, $v = p/(m_e\gamma)$, and the "collision frequency" associated with the whistler-electron interaction:

$$\frac{1}{\tau} = \frac{\pi}{4}\Omega_e^2 \left|\frac{v_{ph} - v\cos\theta}{v_{ph}}\right| \hat{\mathcal{B}}_\omega \tag{6}$$

$\hat{\mathcal{B}}_\omega$ is the wave spectral energy density at the frequency ω, normalized to the magnetic field energy density, $B^2/(2\mu_0)$, and Ω_e is the electron cyclotron frequency, $\Omega_e = eB/m_e$.

The frequency of a wave that interacts with an electron with given momentum (p, θ) is determined by the resonance condition

$$\omega - k_\parallel p_\parallel/(m_e\gamma) = \Omega_e/\gamma. \tag{7}$$

$p_\parallel = p\cos\theta$ is the momentum component parallel to the background magnetic field, and $k_\parallel$ is the parallel wave vector component. It basically states that the electron's gyrofrequency equals the Doppler-shifted wave frequency in the electron frame. Since the whistler wave dispersion relation only allows wave propagation for frequencies below the local electron cyclotron frequency, $\omega < \Omega_e$, it follows that electrons and waves must propagate into opposite directions.

The main effect of resonant electron—whistler interaction is pitch-angle scattering of the electrons in the reference frame of the waves, leading to the formation of "kinetic shells" as in the solar wind model of Isenberg et al. (2001) who studied the interaction of protons with proton cyclotron waves. Figure 3 shows the kinetic shells for (a) high and (b) low electron Alfvén speeds, $v_{A,e} = B/\sqrt{\mu_0 N_e m_e}$. The solar wind corresponds to the case of low wave phase speeds, (b). Due to the small difference between wave and plasma reference frames the resonant interaction with whistlers mainly leads to pitch-angle scattering of the electrons.

Figure 4 shows the resulting solar wind electron VDF in the model of Vocks et al. (2005) that includes whistler wave scattering. The whistler wave spectrum is based on Salem (2000), which is a compilation of data from different instruments onboard the WIND spacecraft (Mangeney et al. 2001). Each 1% of the total wave power is attributed to whistlers propagating sunward and anti-sunward along the magnetic field. The simulation box extends from the transition region in the solar atmosphere through the corona over 3.9 AU

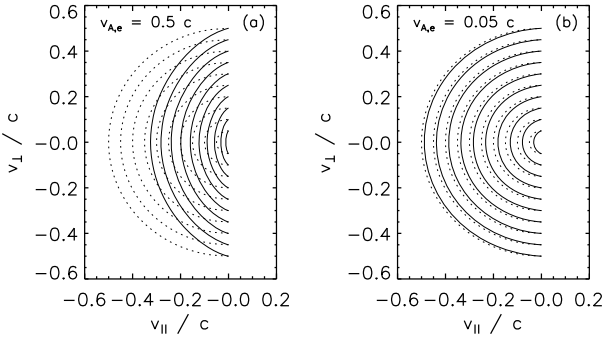

Fig. 3 Kinetic shells for electrons in plasmas with different electron Alfvén speeds (*solid lines*). Isolines for a Maxwellian VDF are shown for comparison (*dotted lines*)

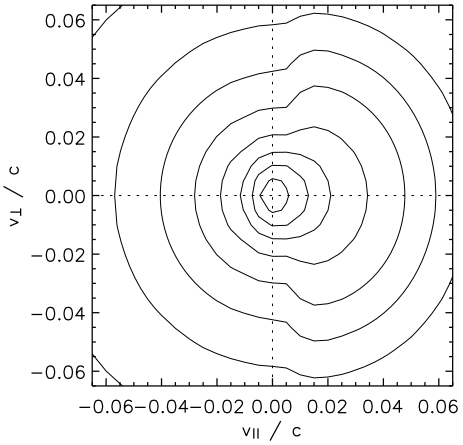

Fig. 4 Solar wind electron VDF from the simulation of Vocks et al. (2005) at a solar distance of 0.96 AU

along the Parker spiral into interplanetary space. This model is much more realistic than exospheric models. A thermal core, an anisotropy resembling the strahl, and an isotropic halo are clearly visible. From the resonance condition, (7), it follows that sunward propagating waves scatter electrons out of the strahl into the halo, and the anti-sunward waves provide an isotropic distribution for $v_\parallel < 0$. The step at $v_\parallel = 0$ is an artifact due to the weak scattering quasilinear theory provides at this speed for waves parallel to the magnetic field.

So whistler waves are indeed capable of scattering electrons out of the strahl into the anti-solar direction, overcoming the focusing effect of the mirror force. Scattering of strahl electrons into the halo is also found in observational studies of solar wind electron VDFs (Maksimovic et al. 2005; Pagel et al. 2007; Štverák et al. 2009). So it has to be concluded that scattering of electrons by whistler waves plays an important role in the evolution of solar wind VDFs.

3 Scattering of Solar Energetic Electrons

In the previous section the influence of whistler wave scattering on solar wind electron distributions has been discussed for quiet solar conditions. Those VDFs represent a stationary state. But interplanetary space can be highly dynamic. Solar flares are well known for producing energetic electrons and releasing them into the solar wind. These electrons are also

scattered by whistler waves, thus it is worthwhile to investigate this influence on energetic electron propagation.

Flare-generated energetic electrons lead to the emission of X-rays and radio waves in the corona, and are recorded in-situ by spacecraft at 1 AU solar distance. Since electrons with higher energies move faster than those with lower energies, they arrive earlier at 1 AU. This velocity dispersion allows for a determination of path lengths and release times of the electrons.

Since scattering of electrons by whistler waves also depends on energy, this effect should alter the inferred release times. And indeed observations show a difference between X-ray onset times and release times of up to 10 min (Krucker et al. 2007). So the question arises whether it is the same electron population that emits X-rays and is recorded in interplanetary space, and if so, whether the electrons are delayed due to scattering in the solar wind, or they are somehow stored in the corona prior to release.

But on the other hand, the analysis of electron arrival times seems to be in agreement with the assumption of free propagation (Claßen et al. 2003). So it has to be studied to what extent energetic electrons are delayed due to scattering in the solar wind, and how this depends on energy. Such a study has been done by Vocks and Mann (2009). Their simulation box extends from the flare site in the corona over 3 AU into interplanetary space. The flare injects electrons with a distribution based on RHESSI (Lin et al. 2003) observations. The flare electrons have a density of 10^{11} m^{-3}, temperature of 10 MK, a $\kappa = 4$ distribution, a low-energy cutoff at 20 keV, and rise and fall times of each 60 s. The whistler wave spectrum is the same as in the solar wind model shown in Fig. 4.

Figure 5 shows resulting electron VDFs in interplanetary space. The first plot displays the initial VDF, a $\kappa = 30$ distribution that is close to a Maxwellian, but avoids its steep phase-space gradients at higher energies that cause numerical problems. Then the flare electrons arrive, first at high and then at lower energies. The pitch-angle diffusion caused by the whistler waves is clearly visible. After the flare, the model heliosphere remains filled with high-energy electrons for days, thus resembling the super-halo component found in solar wind electron VDFs under quiet conditions (Lin 1998).

Since whistler wave phase speeds are low in the solar wind, their main effect on the electron distribution is pitch-angle diffusion, cf. Fig. 3b. So it might be tempting to simplify the diffusion equation (4) to pure pitch-angle diffusion and save computer costs. Figure 6 shows the delay of electron arrival times as compared to free propagation for different models. A test run without whistlers shows small residual delays of less than 15 s due to the finite numerical accuracy. The earlier arrival at low energies is due to Coulomb collisions. The mechanism that leads to early arrival is explained below. Pure pitch-angle scattering leads to delays of up to 50 s, with a strong energy dependence that might lead to wrong conclusions about travel path lengths. This is still much less than the observed delays of 10 min. But surprisingly, the results for a model that considers the full diffusion equation hardly differ from the free propagation ones.

The reason for this is the weak but finite diffusion in momentum space. There are strong gradients in the electron VDF at the energy where the flare electrons just have arrived, as can be seen in Fig. 5. Electrons diffuse to lower momentum p, that is to lower energy. As a consequence, the arrival time at this lower energy seems to be earlier. Reid and Kontar (2010) have studied a similar effect due to electron scattering on Langmuir waves. So the delay due to pitch-angle diffusion just compensates the earlier arrival due to energy diffusion. This explains the observations of quasi-free electron propagation and arrival. But the details depend on the whistler phase speeds in the solar wind, and thus on local plasma conditions. So it has to be concluded that scattering by whistlers does influence energetic electron propagation, but the two main effects compensate each other.

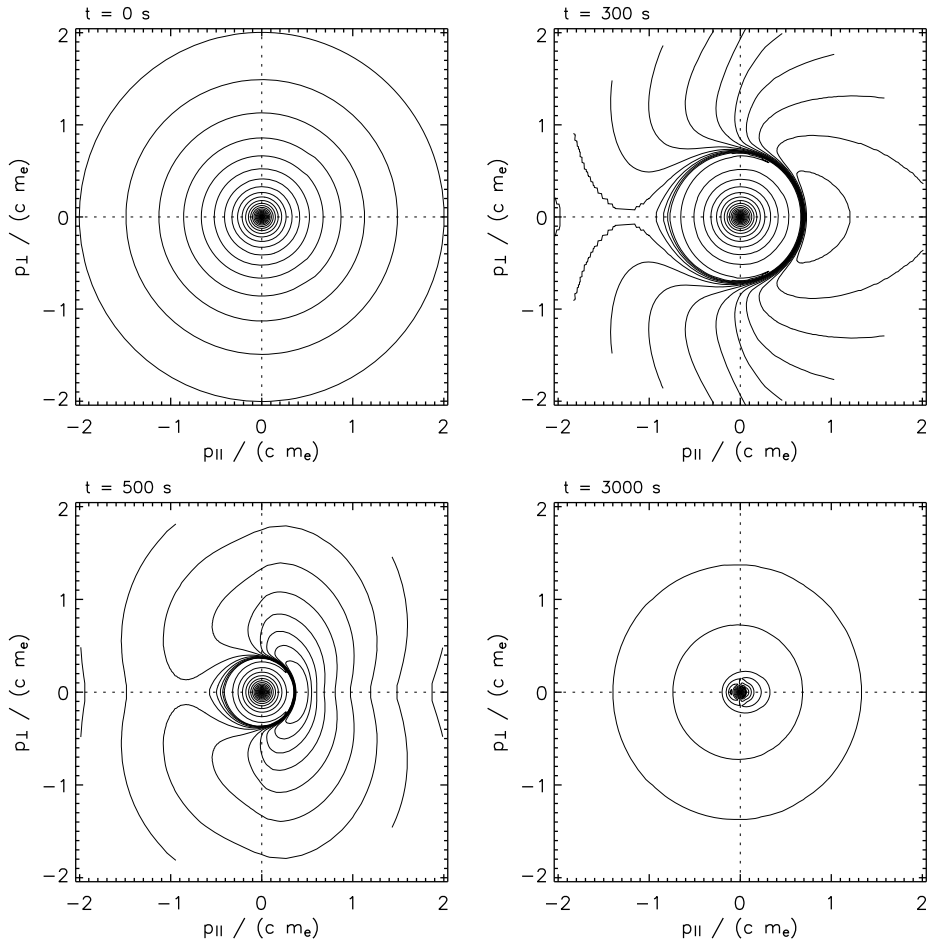

Fig. 5 Solar wind electron distributions at a distance of 0.35 AU for different simulation times. The isolines would be equidistant for a Maxwellian VDF

4 Generation of Suprathermal Electrons under Quiet Solar Conditions

In the previous sections electron scattering by whistler waves has been studied in the solar wind. But it also plays an important role in the corona. The solar wind plasma is characterized by relatively low whistler wave phase speeds, so that their main effect on electrons is pitch-angle diffusion, although diffusion in energy or momentum has been found not to be negligible. But in the solar corona this is different. There, the wave phase speeds are higher, and the "kinetic shells" considerably differ from isotropic distributions, cf. Fig. 3a.

Under such conditions, electrons can be scattered from low $v_\parallel$ to high $v_\perp$, and thus gain energy. It follows from the resonance condition, (7), that this sketch for electrons with $v_\parallel < 0$ is valid for waves that propagate anti-sunward, $k_\parallel > 0$. These electrons eventually reach positive $v_\parallel$, but they can be scattered back in interplanetary space and undergo multiple such cycles, thus leading to the formation of suprathermal tails. The necessary wave power in the corona can be seen as the high-frequency tail of a wave spectrum as discussed for coronal

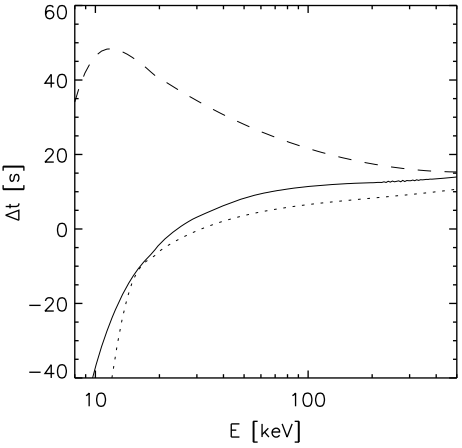

Fig. 6 Delay of electron arrival times for free propagation (*solid line*), pure pitch-angle diffusion (*dashed line*), and the full diffusion equation (*dotted line*)

heating (Cranmer et al. 1999; Vocks 2002). Not only left-hand, but also right-hand polarized waves, i.e. whistlers, should be present.

One might object that the bulk of thermal electrons absorbs this little whistler wave energy. But from the resonance condition, (7), it follows that higher electron speeds correspond to lower resonance frequencies. If a wave travels upwards in the corona, it sees a decreasing local magnetic field and thus electron cyclotron resonance frequency. So if its frequency is initially below all electron resonance frequencies, it will eventually resonate with the electrons with highest speeds. So it can lead to the formation of suprathermal tails of the electron VDF without being absorbed by thermal electrons that have much higher resonance frequencies. This mechanism has been explained in detail by Vocks and Mann (2003), where the electron-whistler interaction indeed leads to the formation of suprathermal tails in the corona.

This was a model for the open magnetic structure of a coronal funnel. Vocks et al. (2008) have run a more detailed investigation for the closed plasma volume of a coronal loop. A whistler wave power-law spectrum with a spectral index of 1.3 was fed into both loop footpoints. The waves thus propagate through the loop in both directions. The wave energy was chosen to be in agreement with being the high-frequency tail of a spectrum responsible for coronal heating. The loop geometry was based on potential magnetic field extrapolations (Seehafer 1978; Sakurai 1982; Aurass et al. 2005) of a photospheric magnetic field data set. A hydrostatic density model was assumed inside the loop. The simulation box had its borders at both footpoints in the cooler and denser transition region. The boundary conditions for the electron VDF both in space and momentum have been chosen in agreement with a $\kappa = 80$ distribution, that is very close to a Maxwellian in order to avoid artificially injecting suprathermal electrons.

The resulting electron VDFs at the loop footpoints are shown in Fig. 7. The regions with high isoline density mark boundaries between electrons that have entered the loop at the footpoints and electrons that are trapped inside the loop. The effect of the whistler waves, the formation of "kinetic shells", is clearly visible. Inside the loop, the electron VDFs become more isotropic, as whistler phase speeds decrease. At the loop top a core-halo distribution has formed, as can be seen in Fig. 8. The VDF is not symmetric since the loop itself is asymmetric. The thermal core extends up to energies of 5 keV due to high density and thus efficient Coulomb collisions inside the loop. So at loop footpoints high wave phase speeds lead to electron acceleration, and at the loop top low wave phase speeds lead to pitch-angle

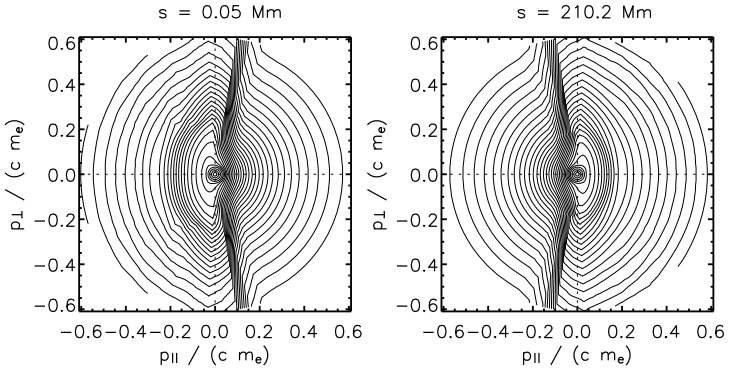

Fig. 7 Electron VDF at both loop footpoints in the model of Vocks et al. (2008)

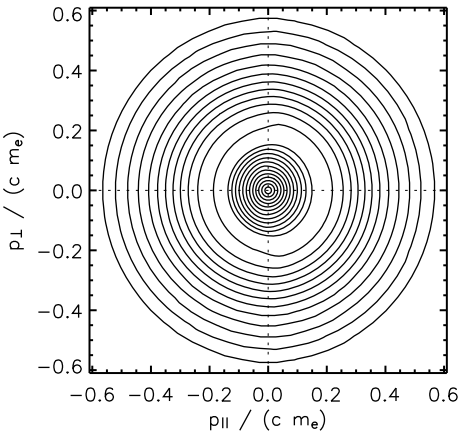

Fig. 8 Electron VDF at the loop top

scattering of the electrons. Electrons are trapped inside the loop due to the magnetic mirror effect of the higher field at the footpoints. As a consequence, electrons can be reflected inside the loop between footpoints and undergo multiple acceleration cycles.

The model does find the formation of a suprathermal tail of the electron VDF. Figure 9 shows a cut through the pitch-angle averaged VDF at the loop top. It can be fitted with a power law that corresponds to a $\kappa = 1.8$. At higher energy, the VDF falls off, but this is due to the high-energy boundaries of the simulation box. This model run demonstrates that resonant interaction between electrons and whistler waves is capable of producing suprathermal tails, even under quiet solar conditions without any flare activity.

5 Summary and Conclusions

Fluid models that are based on the assumption of particle VDFs close to a Maxwellian cannot resolve all physical processes in a plasma. The condition of a nearly Maxwellian VDF is often not met in the solar wind, strong deviations from this simple distribution are observed for both protons and electrons. Thus, a kinetic description is needed, in the solar corona as well as in the wind.

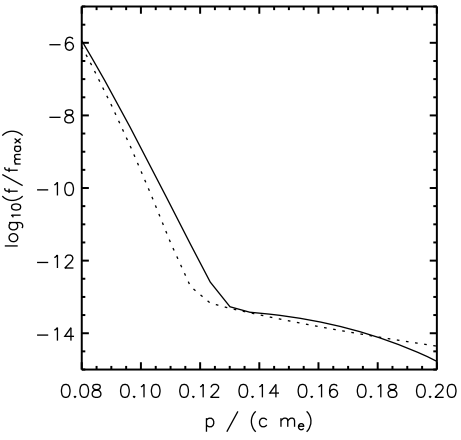

Fig. 9 Pitch-angle averaged electron VDF at the loop top for energies up to 10 keV. The *dotted line* is a Maxwellian + kappa distribution with $\kappa = 1.8$ and density $N_\kappa = 3 \times 10^{-9}$ of the Maxwellian

The importance of electron diffusion in interplanetary space has been shown. Coulomb collisions are too weak to provide this diffusion, but resonant interaction between electrons and whistler waves can. The inclusion of resonant interaction with whistlers waves in a kinetic solar wind model leads to good agreement with observed distributions, including core, halo, and strahl populations.

Diffusion processes are also important for the propagation of flare electrons in the solar wind after their release in the corona. Observations of quasi-free propagation seem to be surprising given that scattering must occur, but detailed numerical studies show that the effects of a delay due to pitch-angle diffusion and earlier arrival times due to energy diffusion just compensate each other. The details of course depend on the plasma background conditions and may vary with time. The same numerical studies showed that energetic electrons can persist in the heliosphere for days, forming an isotropic distribution that resembles the super-halo observed under quiet solar conditions (Lin 1998).

But resonant scattering of electrons by whistler waves not just affects their propagation. In a plasma with high wave phase speeds, electrons can be brought from low speeds parallel to the magnetic field to high speeds perpendicular to it, following the "kinetic shells" that the waves try to establish in the plasma. These results demonstrate that the solar, or any stellar, corona is capable of continuously producing suprathermal electrons even under quiet conditions without flare activity.

These examples of solar corona and wind models show that kinetic processes play an important role. They are necessary for a correct representation of the physical processes that affect the bulk properties of space plasmas.

Acknowledgements This work was supported by the German *Deutsche Forschungsgemeinschaft, DFG* project number MA 1376/17-1. I would like to thank Prof. G. Mann for many stimulating discussions.

References

H. Aurass, G. Rausche, G. Mann, A. Hofmann, Astron. Astrophys. **435**, 1137 (2005)
H.T. Claßen, G. Mann, A. Klassen, H. Aurass, Astron. Astrophys. **409**, 309 (2003)
S.R. Cranmer, G.B. Field, J.L. Kohl, Astrophys. J. **518**, 937 (1999)
J.C. Dorelli, J.D. Scudder, J. Geophys. Res. **108** (2003). doi:10.1029/2002JA009484
P. Hackenberg, E. Marsch, G. Mann, Astron. Astrophys. **360**, 1139 (2000)

C.M. Hammond, W.C. Feldman, D.J. McComas, J.L. Phillips, R.J. Forsyth, Astron. Astrophys. **316**, 250 (1996)
V.H. Hansteen, E. Leer, J. Geophys. Res. **100**, 21577 (1995)
J.-S. He, C.-Y. Tu, E. Marsch, Sol. Phys. **250**, 147 (2008)
Y.Q. Hu, R. Esser, S.R. Habbal, J. Geophys. Res. **105**, 5093 (2000)
P.A. Isenberg, A.M. Lee, V.J. Hollweg, J. Geophys. Res. **106**, 5649 (2001)
K. Jockers, Astron. Astrophys. **6**, 219 (1970)
C.F. Kennel, F. Engelmann, Phys. Fluids **9**, 2377 (1966)
J.L. Kohl, G. Noci, E. Antonucci, G. Tondello, M.C.E. Huber, R. Cranmer, L. Strachan, A.V. Panasyuk, L.D. Gardner, M. Romollo, S. Fineschi, D. Dobrzycka, J.C. Raymond, P. Nicolosi, O.H.W. Siegmund, D. Sparado, C. Benna, A. Ciaravella, S. Giordano, S.R. Habbal, M. Karovska, X. Li, R. Martin, J.G. Michels, A. Mondigliani, G. Naletto, R.H. O'Neal, C. Pernechele, G. Poletto, P.L. Smith, R.M. Suleiman, Astrophys. J. **501**, L121 (1998)
S. Krucker, E.P. Kontar, S. Christe, R.P. Lin, Astrophys. J. **663**, L109 (2007)
S. Landi, F. Pantellini, Astron. Astrophys. **400**, 769 (2003)
Ø. Lie-Svendsen, V.H. Hansteen, E. Leer, J. Geophys. Res. **102**, 4701 (1997)
R.P. Lin, Space Sci. Rev. **16**, 189 (1974)
R.P. Lin, K.A. Anderson, S. Ashford, C. Carlson, D. Curtis, R. Ergun, D. Larson, J. McFadden, M. McCarthy, G.K. Parks, H. Rème, J.M. Bosqued, J. Coutelier, F. Cotin, C. D'Uston, K.-P. Wenzel, T.R. Sanderson, J. Henrion, J.C. Ronnet, G. Paschmann, Space Sci. Rev. **71**, 125 (1995)
R.P. Lin, Space Sci. Rev. **86**, 61 (1998)
R.P. Lin, S. Krucker, G.J. Hurford, D.M. Smith, H.S. Hudson, G.D. Holman, R.A. Schwartz, B.R. Dennis, G.H. Share, R.J. Murphy, A.G. Emslie, C. Johns-Krull, N. Vilmer, Astrophys. J. **595**, L69 (2003)
M. Maksimovic, V. Pierrard, P. Riley, Geophys. Res. Lett. **24**, 1151 (1997)
M. Maksimovic, I. Zouganelis, J.-Y. Chaufray, K. Issautier, E.F. Scime, J.E. Littleton, E. Marsch, D.J. McComas, C. Salem, R.P. Lin, H. Elliott, J. Geophys. Res. **110**, 9104 (2005)
A. Mangeney, C. Salem, P.L. Veltri, B. Cecconi, in *Intermittency in the Solar Wind Turbulence and the Haar Wavelet Transform*, Sheffield Space Plasma Meeting: Multipoint Measurements versus Theory. ESA, vol. SP-492 (2001), p. 53
E. Marsch, Nonlinear Process. Geophys. **5**, 111 (1998)
E. Marsch, C.-Y. Tu, J. Geophys. Res. **106**, 227 (2001)
E. Marsch, Living Reviews in Solar Phys. **3** (2006)
T. Nieves-Chinchilla, A.F. Viñas, J. Geophys. Res. **113** (2008). doi:10.1029/2007JA012703
L. Ofman, J. Geophys. Res. **109**, 7102 (2004)
M.J. Owens, N.U. Crooker, N.A. Schwadron, J. Geophys. Res. **113**, 11104 (2008)
C. Pagel, S.P. Gary, C.A. de Koning, R.M. Skoug, J.T. Steinberg, J. Geophys. Res. **112**, 4103 (2007)
V. Pierrard, M. Maksimovic, J. Lemaire, J. Geophys. Res. **104**, 17021 (1999)
V. Pierrard, M. Maksimovic, J. Lemaire, J. Geophys. Res. **106**, 29305 (2001)
W.G. Pilipp, H. Miggenrieder, M.D. Montgomery, K.H. Mühlhäuser, H. Rosenbauer, R. Schwenn, J. Geophys. Res. **92**, 1075 (1987)
H.A. Reid, E.P. Kontar, Astrophys. J. **721**, 864 (2010)
T. Sakurai, Sol. Phys. **76**, 301 (1982)
C. Salem, PhD thesis, Univ. Paris (2000)
J.D. Scudder, Astrophys. J. **398**, 299 (1992a)
J.D. Scudder, Astrophys. J. **398**, 319 (1992b)
N. Seehafer, Sol. Phys. **58**, 215 (1978)
Š. Štverák, M. Maksimovic, P.M. Trávníček, E. Marsch, A.N. Fazakerley, E.F. Scime, J. Geophys. Res. **114**, 5104 (2009)
C. Vocks, Astrophys. J. **568**, 1017 (2002)
C. Vocks, G. Mann, Astrophys. J. **593**, 1134 (2003)
C. Vocks, C. Salem, R.P. Lin, G. Mann, Astrophys. J. **627**, 540 (2005)
C. Vocks, G. Mann, G. Rausche, Astron. Astrophys. **480**, 527 (2008)
C. Vocks, G. Mann, Astron. Astrophys. **502**, 325 (2009)
I. Zouganelis, M. Maksimovic, N. Meyer-Vernet, H. Lamy, K. Issauthier, Astrophys. J. **606**, 542 (2004)